This document is a preprint of: I. Gaspar, M. Matthe, N. Michailow, L. Mendes, D. Zhang and G. Fettweis, "Frequency-shift Offset-QAM for GFDM," in Communication Letters (CommL), vol. PP, no. 99, Dec 2015. DOI:10.1109/LCOMM.2015.2445334

Frequency-shift Offset-QAM for GFDM

Ivan Gaspar, Maximilian Matthé, Nicola Michailow, Luciano Leonel Mendes, Dan Zhang and Gerhard Fettweis

***Abstract*—This paper presents a novel perspective to apply the offset quadrature amplitude modulation (OQAM) scheme on top of the multicarrier waveform termed Generalized Frequency Division Multiplexing (GFDM). The conventional time-shift OQAM is described for GFDM and, with the introducing of the general use of unitary transform, an interesting counterpart, i.e., frequency-shift OQAM, is proposed. The conventional long prototype pulse with time-shift of one half subsymbol becomes a short prototype pulse with frequency-shift of one half subcarrier. The frequency-shift OQAM scheme offers advantages such as low out-of-band emission and low implementation complexity. The concept can be applied to the broader scope of filtered OFDM without penalties in terms of performance in time variant frequency-selective channels.**

***Index Terms*—Offset-QAM, multicarrier modulation, GFDM**

I. Introduction

Generalized Frequency Division Multiplexing (GFDM) is a candidate waveform that has been investigated as a component in the physical layer (PHY) of future wireless communication systems [1], [2]. In particular, GFDM can use time-frequency localization (TFL) of the transmit signal to address spectral agility and aggregation of carriers with adaptation of the prototype filter and resource grid.

GFDM supports the use of standard Quadrature Amplitude Modulation (QAM) modulation [3], but the Balian-Low theorem implies that good TFL results in a distorted reconstruction of the complex valued-symbols at Nyquist rate [4]. Either advanced receivers can be designed to mitigate self-interference [5], or the use of Offset QAM (OQAM) can be exploited to address non-orthogonal conditions. A version of time-shifted OQAM-GFDM (TS-OQAM-GFDM) has already been shown to be free of self-generated interference [6], achieving the same symbol error rate (SER) performance of orthogonal waveforms under mobile channels. The OQAM mapping also minimizes the singularity problems with the modulation matrix when even number of subcarriers and subsymbols are employed [3]. However, OQAM applied in time-domain results in a time-shift between the two real-valued data sequences and leads to overlapping subsymbols. This means that the subsymbol by subsymbol detection cannot be achieved, since the entire GFDM frame is required to recover the self-interference free data sequence. Additionally, using time-shift OQAM with half-Nyquist filters, which are not intersymbol interference (ISI)-free when unmatched, reduces the efficient use of simple guard subsymbols to smooth the block boundaries to reduce out-of-band (OOB) radiation of a GFDM block [1].

This paper extends the use of OQAM by incorporating unitary transformations and selecting an interesting corner case that allows to explore the duality between time and frequency domains to design the prototype filter, named frequency-shift OQAM-GFDM (FS-OQAM-GFDM). In this sense, in contrast to classic literature [7], the impulse and frequency responses of the prototype filter are exchanged. It will be shown that a half-Nyquist pulse, limited to the width of two subsymbols, requires a frequency-shift of one half subcarrier, instead of a time-shift of one half subsymbol. It turns out that the absence of a time-shift allows the FS-OQAM-GFDM to better use null subsymbols [1] to achieve low OOB emission and the more sparse impulse response can simplify the hardware implementation.

When applied to general filtered OFDM modulation, especially those aiming at short pulses at the cost of noise enhanced bi-orthogonal pulse design [8], the well localized impulse response used in FS-OQAM-GFDM is also useful to reduce the system latency, by allowing subsymbol by subsymbol demodulation. This feature is very interesting in cases where constant amplitude differential modulation, such as differential quadrature phase shifting, can be used without equalization, allowing for low latency Tactile Internet to provide high Quality of Experience (QoE) or low-complex solutions for Machine-to-Machine (M2M) communications with low latency.

II. GFDM background

GFDM [1] is a filtered multicarrier modulation where a prototype pulse $g[n]$ is circularly shifted in time and frequency to produce the pulse shapes

$$g_{k,m}[n] = g[(n - mK) \bmod N]e^{j2\pi \frac{k}{K} n}, \tag{1}$$

where $n = 0, 1, \ldots, N-1$ is the time index, K and M are respectively the number of subcarriers and subsymbols and $N = MK$.

Assume $d_{k,m}$ to be the complex-valued data symbol carried by the kth subcarrier and mth subsymbol. The GFDM signal is given by

$$x[n] = \sum_{m=0}^{M-1} \sum_{k=0}^{K-1} d_{k,m} g_{k,m}[n]. \tag{2}$$

The pulse shapes for every subcarrier and subsymbol can be organized in a modulation matrix, given by

$$\mathbf{A} = [\mathbf{g}_{0,0} \ \cdots \ \mathbf{g}_{K-1,0} \ \mathbf{g}_{0,1} \ \cdots \ \mathbf{g}_{K-1,M-1}], \tag{3}$$

Manuscript received XXX XX, XXXX; revised XXXX XX, XXXX; accepted XXXX XX, XXXX. Date of publication: XXX XX, XXXX.

Ivan Gaspar, Maximilian Matthé, Nicola Michailow, Dan Zhang and Gerhard Fettweis are with Vodafone Chair Mobile Communications Systems, TU Dresden, Germany. e-mail: {first name.last name}@ifn.et.tu-dresden.de

Luciano Leonel Mendes is with Instituto Nacional de Telecomunicações (Inatel), Sta. Rita do Sapucai, MG, Brazil. e-mail: luciano@inatel.br

This work has been performed in the framework of the FP7 project ICT-318555 5GNOW, which is partly funded by the European Union. The authors would like to thank CNPq - Brasil for partially funding the work presented in this paper.

This document is a preprint of: I. Gaspar, M. Matthe, N. Michailow, L. Mendes, D. Zhang and G. Fettweis, "Frequency-shift Offset-QAM for GFDM," in Communication Letters (CommL), vol. PP, no. 99, Dec 2015. DOI:10.1109/LCOMM.2015.2445334

where $\mathbf{g}_{k,m}$ is a column vector containing the samples from $g_{k,m}[n]$. The GFDM transmit vector is given by

$$\mathbf{x} = \mathbf{A}\mathbf{d} \tag{4}$$

where $\mathbf{d}$ is a column vector with all data symbols $d_{k,m}$.

III. Time-shift OQAM for GFDM

In TS-OQAM-GFDM, interference-free transmission can be achieved transmitting the real and imaginary parts of the data symbol, $d_{k,m} = d^{(\mathrm{i})}_{k,m} + j d^{(\mathrm{q})}_{k,m}$, using symmetric, real-valued, half Nyquist prototype filters with offset of $K/2$ samples from each other and phase rotation of $\frac{\pi}{2}$ radians among adjacent subcarriers and subsymbols, given by

$$g^{(\mathrm{i})}_{k,m}[n] = j^k g_{k,m}[n], \tag{5}$$
$$g^{(\mathrm{q})}_{k,m}[n] = j^{k+1} g_{k,m+\frac{1}{2}}[n], \tag{6}$$

which leads to

$$x[n] = \sum_{m=0}^{M-1}\sum_{k=0}^{K-1} d^{(\mathrm{i})}_{k,m} g^{(\mathrm{i})}_{k,m}[n] + \sum_{m=0}^{M-1}\sum_{k=0}^{K-1} d^{(\mathrm{q})}_{k,m} g^{(\mathrm{q})}_{k,m}[n]. \tag{7}$$

Assuming a flat and noiseless channel, a matched filtering operation can recover the received signal $y[n] = x[n]$ as follows

$$\hat{d}^{(\cdot)}_{k,m} = \Re\left\{ y[n] \circledast g^{(\cdot)*}_{k,m}[-n] \right\}|_{n=0}, \tag{8}$$

where $\circledast$ denotes circular convolution with period N. Note that real-orthogonality is given by the projection between any m'th subsymbol and the k'th subcarrier at all k, m, i.e

$$\Re\left\{ g^{(\mathrm{i})}_{k,m}[n] \circledast g^{(\mathrm{i})*}_{k',m'}[-n] \right\}\Big|_{n=0} = \delta[k,m]\delta[k',m'], \tag{9}$$
$$\Re\left\{ g^{(\mathrm{q})}_{k,m}[n] \circledast g^{(\mathrm{q})*}_{k',m'}[-n] \right\}\Big|_{n=0} = \delta[k,m]\delta[k',m'], \tag{10}$$
$$\Re\left\{ g^{(\mathrm{i})}_{k,m}[n] \circledast g^{(\mathrm{q})*}_{k',m'}[-n] \right\}\Big|_{n=0} = 0, \tag{11}$$
$$\Re\left\{ g^{(\mathrm{q})}_{k,m}[n] \circledast g^{(\mathrm{i})*}_{k',m'}[-n] \right\}\Big|_{n=0} = 0, \tag{12}$$

and that the symmetric half-Nyquist bandlimited filters [7] assure zero ISI at any m'th subsymbol and produce null imaginary interference at any k'th neighboring subcarrier. Hence, the phase rotation aligns the components into a null intercarrier interference (ICI) arrangement.

IV. Matrix model and unitary transformation

The transmitted sequence (7) can be compactly written as

$$\mathbf{x} = \mathbf{A}^{(\mathrm{i})}\mathbf{d}^{(\mathrm{i})} + \mathbf{A}^{(\mathrm{q})}\mathbf{d}^{(\mathrm{q})}, \tag{13}$$

where the first/second term of (13) corresponds to the first/second double sum in (7) and the columns of the matrix $\mathbf{A}^{(\mathrm{i})}$ and $\mathbf{A}^{(\mathrm{q})}$ carry $\mathbf{g}^{(\mathrm{i})}_{k,m}$ and $\mathbf{g}^{(\mathrm{q})}_{k,m}$, respectively.

Observing that

$$\left(g^{(\cdot)}_{k,m}[n] \circledast g^{(\cdot)*}_{k',m'}[-n] \right)\Big|_{n=0} = \left(\mathbf{g}^{(\cdot)}_{k',m'} \right)^H \mathbf{g}^{(\cdot)}_{k,m}, \tag{14}$$

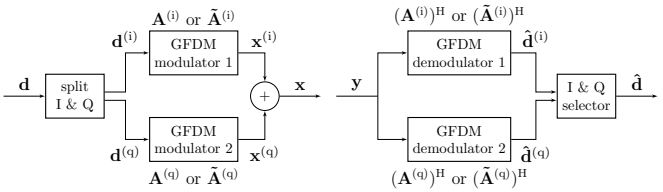

Fig. 1: Block structure of the time-shift or frequency-shift OQAM-GFDM.

the conditions given in (9) and (11) are equivalent to

$$\Re\left\{ \left(\mathbf{A}^{(\mathrm{i})}\right)^{\mathrm{H}} \mathbf{A}^{(\mathrm{i})} \right\} = \Re\left\{ \left(\mathbf{A}^{(\mathrm{q})}\right)^{\mathrm{H}} \mathbf{A}^{(\mathrm{q})} \right\} = \mathbf{I}_N \tag{15}$$
$$\Re\left\{ \left(\mathbf{A}^{(\mathrm{i})}\right)^{\mathrm{H}} \mathbf{A}^{(\mathrm{q})} \right\} = \Re\left\{ \left(\mathbf{A}^{(\mathrm{q})}\right)^{\mathrm{H}} \mathbf{A}^{(\mathrm{i})} \right\} = \mathbf{0}_N. \tag{16}$$

This matrix model is very helpful to show that the orthogonality condition (15) is valid under any unitary transform $\mathbf{U}_N$ being applied to the transmit matrix due to

$$\left(\mathbf{U}^{\mathrm{H}}_N \mathbf{A}^{(\cdot)}\right)^{\mathrm{H}} \mathbf{U}^{\mathrm{H}}_N \mathbf{A}^{(\cdot)} = \left(\mathbf{A}^{(\cdot)}\right)^{\mathrm{H}} \mathbf{A}^{(\cdot)}, \tag{17}$$

and this is a key property that can allow the introduction of new classes of offset QAM, where a first proposal is presented next.

V. Frequency-shift OQAM for GFDM

Considering the unitary discrete Fourier transform (DFT) transform matrix $\mathbf{W}_N$ with $[\mathbf{W}_N]_{i,l} = 1/\sqrt{N} e^{-j2\pi \frac{il}{N}}$, two new precoding matrices can be constructed from $\mathbf{A}^{(\mathrm{i})}$ and $\mathbf{A}^{(\mathrm{q})}$ as

$$\begin{aligned} \tilde{\mathbf{A}}^{(\mathrm{i})} &= \mathbf{W}^{\mathrm{H}}_N \mathbf{A}^{(\mathrm{i})}, \\ \tilde{\mathbf{A}}^{(\mathrm{q})} &= \mathbf{W}^{\mathrm{H}}_N \mathbf{A}^{(\mathrm{q})}. \end{aligned} \tag{18}$$

Using them, the proposed scheme is achieved

$$\mathbf{x} = \tilde{\mathbf{A}}^{(\mathrm{i})}\mathbf{d}^{(\mathrm{i})} + \tilde{\mathbf{A}}^{(\mathrm{q})}\mathbf{d}^{(\mathrm{q})} \tag{19}$$

followed by the corresponding demodulation equation

$$\hat{\mathbf{d}} = \Re\{(\tilde{\mathbf{A}}^{(\mathrm{i})})^{\mathrm{H}}\mathbf{y}\} + j\Re\{(\tilde{\mathbf{A}}^{(\mathrm{q})})^{\mathrm{H}}\mathbf{y}\}. \tag{20}$$

The relation given in (18) effectively suggests the signal modulation introduced into (19) is equivalent to applying the conventional OQAM modulation in frequency domain and then transforming the result back into the time domain. Therefore, it is labeled as FS-OQAM-GFDM (Fig. 1). More explicitly, the columns of $\tilde{\mathbf{A}}^{(\mathrm{i})}$ are IDFTs of the columns of $\mathbf{A}^{(\mathrm{i})}$,

$$\tilde{\mathbf{g}}_{k,m+c} = \mathbf{W}^{\mathrm{H}}_N \mathbf{g}_{k,m+c}, \tag{21}$$

with $c \in \{0, 1/2\}$. The entries of $\tilde{\mathbf{g}}_{k,m+c}$ are therefore derived as

$$\begin{aligned}\tilde{g}_{k,m+c}[\tilde{n}] &= \frac{1}{\sqrt{N}} \sum_{n=0}^{N-1} g_{k,m+c}[n] e^{j2\pi \frac{\tilde{n}}{N} n} \\ &= \frac{1}{\sqrt{N}} \sum_{n=0}^{N-1} g[(n-(m+c)K) \bmod N] e^{j2\pi \frac{(kM+\tilde{n})}{N} n} \\ &= \frac{1}{N} \sum_{\nu=0}^{N-1} G[\nu] e^{j2\pi \frac{-(m+c)\nu}{M}} \sum_{n=0}^{N-1} e^{j2\pi \frac{(kM+\tilde{n}+\nu)}{N} n} \\ &= G[(-\tilde{n}-kM) \bmod N] e^{j2\pi \frac{(m+c)\tilde{n}}{M}} \\ &= G[(\tilde{n}+kM) \bmod N] e^{j2\pi \frac{(m+c)\tilde{n}}{M}}, \end{aligned} \tag{22}$$

where $G[n]$ is the frequency representation of the prototype pulse shaping filter $g[n]$ and it is symmetric. The time shift $(m+c)K$ in $g_{k,m+c}[n]$ becomes the frequency offset, while the subcarrier index k becomes the index for time shift in $\tilde{g}_{k,m+c}[\tilde{n}]$.

With this approach, half-Nyquist pulses, which have a rect-like shape with non-null roll-off, are now directly applied as the impulse response in time domain with a sparse response expanding into up to two subsymbols width. Therefore, the necessary shift to obtain the real-orthogonality consists of one half subcarrier and it is applied in the frequency domain. In this scheme, M shall denote the number of subcarriers while K represents the number of subsymbols. Notice that the adjacent subsymbols will differ by a phase shift of $\frac{\pi}{2}$.

VI. Analysis of OOB emission, complexity and SER performance for OQAM-GFDM

One natural question regarding the FS-OQAM-GFDM is the OOB emission, once the spectrum of each subcarrier is not well-localized in the frequency domain. To clarify this point the time and frequency characterizations, normalized to the subsymbol time (T_{SS}) and subcarrier bandwidth (B_{SC}), of FS-OQAM-GFDM and TS-OQAM-GFDM pulses are compared in Fig. 2.

In terms of TFL, the near perfect reconstruction (NPR) filter proposed in [9] is considered for the TS-OQAM-GFDM, while a good candidate for FS-OQAM-GFDM is the Meyer RRC, which uses the Meyer auxiliary function [10] as the argument of a root raised cosine pulse shape defined in time for improved spectrum properties [11].

It is possible to observe that the FS-OQAM-GFDM is much shorter in length, with a maximum span of only 2 subsymbols against several in the TS-OQAM-GFDM case. The FS-OQAM-GFDM symbol structure can benefit from the use of null-subsymbols [1], while in the TS-OQAM-GFDM the long impulse response and the pulse shape design creates signal discontinuities at the block boundaries. Although there might be other cyclic time offset arrangement that can reduce OOB for the considered TS-OQAM-GFDM pulse, it does not have equidistant zeros with interval of one half subsymbol. Hence, in this configuration, TS-OQAM-GFDM cannot outplay the spectrum achieved by FS-OQAM-GFDM, where the OOB radiation is several orders of magnitude

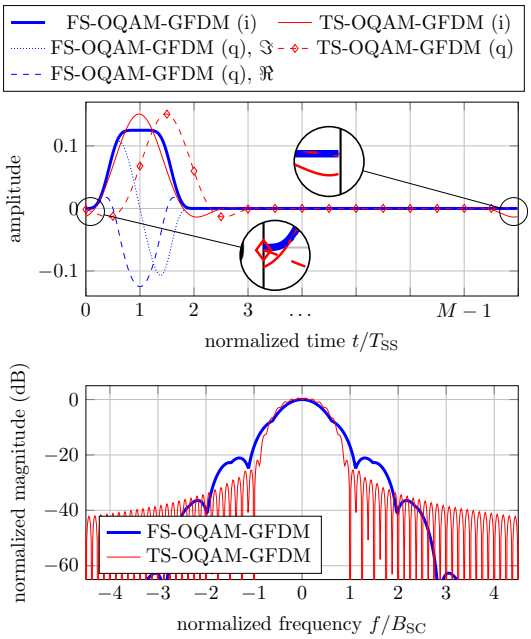

Fig. 2: FS-OQAM-GFDM using Meyer RRC pulse vs TS-OQAM-GFDM using NPR in time and frequency. The figure emphasize the second subsymbol slot impulse response, the first subsymbol slot is left empty to allow smooth block transition.

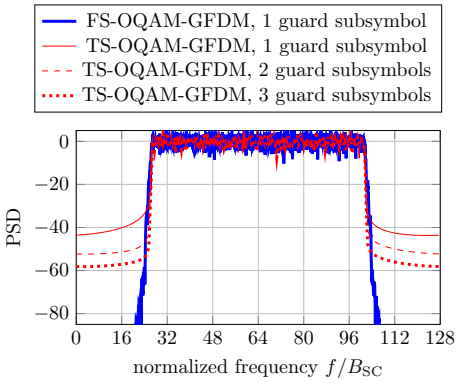

Fig. 3: Simulated spectrum for time-shift with NPR and frequency-shift OQAM-GFDM using Meyer RRC. Burst sequences of 8 subsymbols are transmitted and 75 subcarriers are active.

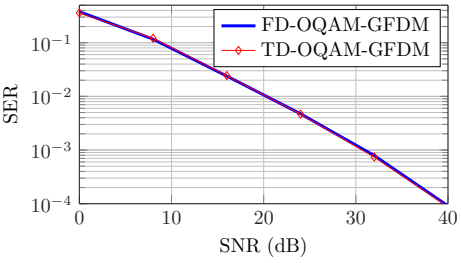

Fig. 4: Simulated SER for time-shift with NPR and frequency-shift OQAM-GFDM using Meyer RRC in a 16 taps channel. Burst sequences of 8 subsymbols are transmitted and 75 subcarriers are active in a frequency-selective channel with exponential decaying gain.

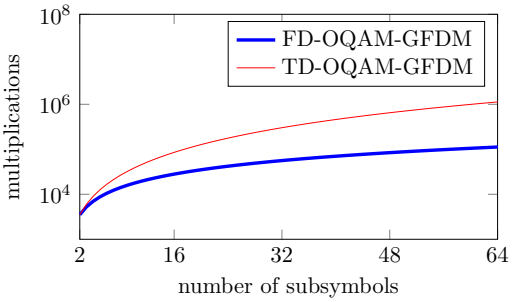

Fig. 5: Complexity assuming 128 subcarriers.

lower. The TS-OQAM-GFDM can slightly outperform the FS-OQAM-GFDM only for frequencies surrounding the adjacent subcarriers and this advantage vanishes when a larger number of subcarriers is transmitted, as shown in Fig. 3.

Lastly, when increasing the number of guard subsymbols at the block boundaries, the TD-OQAM-GFDM resembles the burst case of FBMC/OQAM because the circular pulse shape is no longer observed. This simple consideration proves that the principles of frequency-shift OQAM presented in the context of GFDM also hold for more general filtered OFDM systems.

In order to analyze the performance of the FS-OQAM-GFDM versus the TS-OQAM-GFDM, the symbol error ratio is evaluated in a time variant frequency-selective channel considering perfect synchronization and that the channel impulse response (CIR) is known. A guard interval larger than the CIR is placed between two consecutive bursts to avoid interference. Cyclic convolution with the channel can be emulated by overlapping the tail samples over the initial samples of the GFDM block, allowing for simple zero-forcing (ZF) frequency domain equalization. The tap gains of the simulated channel vary linearly in decibel scale from 0 to -10 dB. Each tap is multiplied by a Rayleigh distributed random variable with parameter $\sigma = 1/\sqrt{2}$. In the simulation, the channel taps are normalized for a unitary gain. Fig. 4 shows that the obtained performance of FS-OQAM-GFDM and TS-OQAM-GFDM are equal.

The low complex GFDM implementation investigated in [12] can be applied to this scheme, which results in the number of multiplications given by $C = 2M(LK + K\log_2(K))$, where $L = 2,\ 3 \ldots M$ is a parameter that represents the maximum length of the prototype filter in terms of subsymbols. For time-shift OQAM-GFDM, the filter impulse response is not well-localized in time domain and it spans to the entire GFDM frame, meaning that $L = M$. For frequency-domain OQAM-GFDM, the prototype filter only spans to the two surrounding half subsymbols, leading to $L = 2$. The complexity for both OQAM-GFDM approaches are compared in Fig. 5, assuming 128 subcarriers.

VII. Conclusion

The main benefit of using OQAM combined with GFDM is the real-orthogonality in the time-frequency grid, where a matched filter receiver can be used without self-interference. In conventional GFDM, the subcarrier filtering can lead to a non-orthogonal system where zero-forcing or minimum mean square error receivers must be used to minimize the self-interference, but with the introduction of noise enhancement and higher complexity.

This paper has shown that OQAM can be applied to GFDM by using frequency-shifts instead of time-shifts. This procedure can bring other advantages, such as easy use of null subsymbols to reduce the out-of-band emission and a reduction of the complexity. These benefits can be achieved because the frequency transfer function of the pulse shaping filter used in the time-shift OQAM case, which typically has a rect-like shape parameterized by a non-zero roll-off factor, becomes the impulse response of the prototype filter adopted by the frequency-shift OQAM scheme. The resulting good time localization limits the overlapping only to the adjacent subsymbols, which can be particularly beneficial to pilot symbol insertion because a frame can be designed where the data and pilot information do not interact with each other. The conversion of the time-shift OQAM scheme to the frequency-shift one is conducted by means of inverse Fourier transform. However, the analysis performed in this paper is not limited to Fourier transform. It can be straightforward extended to any unitary transformation.

References

[1] N. Michailow, M. Matthé, I. Gaspar, A. Navarro Caldevilla, L. L. Mendes, A. Festag, and G. Fettweis, "Generalized Frequency Division Multiplexing for 5th Generation Cellular Networks," *IEEE Transactions on Communications*, 2014.

[2] G. Wunder et al, "5GNOW: non-orthogonal, asynchronous waveforms for future mobile applications," *IEEE Communications Magazine*, vol. 52, no. 2, pp. 97–105, Feb. 2014.

[3] M. Matthé, L. L. Mendes, and G. Fettweis, "GFDM in a Gabor Transform Setting," *IEEE Communications Letters*, 2014.

[4] J. J. Benedetto, C. Heil, and D. F. Walnut, "Gabor Systems and the Balian-Low Theorem," in *Gabor Analysis and Algorithms*, H. G. Feichtinger and T. Strohmer, Eds. Birkhäuser, 1998, ch. 2, pp. 85–122.

[5] I. S. Gaspar, M. N., A. Navarro Caldevilla, E. Ohlmer, S. Krone, and G. Fettweis, "Low Complexity GFDM Receiver Based On Sparse Frequency Domain Processing," in *Vehicular Technology Conference, 2013. VTC Spring 2013, IEEE 77th*, 2013.

[6] H. Lin and P. Siohan, "Multi-carrier modulation analysis and WCP-COQAM proposal," *EURASIP Journal on Advances in Signal Processing*, vol. 2014, no. 1, p. 79, 2014.

[7] H. Bölcskei, "Orthogonal frequency division multiplexing based on offset qam," in *Advances in Gabor Analysis*, ser. Applied and Numerical Harmonic Analysis, H. Feichtinger and T. Strohmer, Eds. Birkhuser Boston, 2003, pp. 321–352.

[8] D. Roque, C. Siclet, and P. Siohan, "A performance comparison of FBMC modulation schemes with short perfect reconstruction filters," in *Telecommunications (ICT), 2012 19th International Conference on*, April 2012, pp. 1–6.

[9] A. Viholainen and M. Bellanger, M. Huchard, "Prototype filter and structure optimization," ser. Tech. Rep., D3.1 of PHYDYAS, FP7-ICT Future Networks, 2008. [Online]. Available: http://www.ict-phydyas.org/delivrables/PHYDYAS-D5-1.pdf

[10] Y. Meyer, "Ondelettes et opérateurs: Ondelettes," ser. Actualités mathématiques. Hermann, 1990.

[11] I. S. Gaspar, L. L. Mendes, N. Michailow, and G. Fettweis, "A Synchronization Technique for Generalized Frequency Division Multiplexing," *EURASIP Journal on Advances in Signal Processing*, vol. 2014, no. 1, pp. 67–76, 2014.

[12] I. Gaspar, M. Matthé, N. Michailow, L. Mendes, D. Zhang, and G. Fettweis, "GFDM Transceiver using Precoded Data and Low-complex Multiplication in Time Domain," *IEEE Wireless Commun. Lett., submitted*. [Online]. Available: http://arxiv.org/abs/1506.03350v1